Acta Cryst. (1987). B43, 305-313

The Determination of the Commensurately Modulated Structure of Tantalum Tetratelluride

BY KLAAS D. BRONSEMA,* SANDER VAN SMAALEN, JAN L. DE BOER, GERRIT A. WIEGERS AND FRANZ JELLINEK

Laboratory of Inorganic Chemistry, Materials Science Centre, University of Groningen, Nijenborgh 16, 9747 AG Groningen, The Netherlands

AND JAN MAHY

University of Antwerp (RUCA), Groenenborgerlaan 171, B-2020 Antwerp, Belgium

(*Received* 12 *November* 1985; *accepted* 24 *July* 1986)

Abstract

The incommensurately modulated structure of tantalum tetratelluride ($TaTe_4$) has been determined by X-ray diffraction on the basis of a $2a \times 2a \times 3c$ supercell. Mo $K\alpha$ radiation, $\lambda = 0{\cdot}71069$ Å, $\mu = 405{\cdot}0\ cm^{-1}$. The space group of the subcell is $P4/mcc$, that of the supercell $P4/ncc$. $a = 6{\cdot}5154\,(5)$, $c = 6{\cdot}8118$ Å, $R_F = 0{\cdot}064$ for 6422 observed reflections. The structure is characterized by $TaTe_4$ chains along the c axis. These chains are modulated in such a way that Ta_3 clusters are formed. The Te atoms respond to the displacements of the Ta atoms, keeping the bonds of the Te dimers, which link the chains, equal in length. The clusters in neighbouring chains are shifted with respect to each other with a phase shift of $\frac{1}{3}$, causing the doubling of the a axis. A simple model is proposed to account for the observed modulations in $NbTe_4$ and $TaTe_4$.

1. Introduction

The polychalcogenides of niobium and tantalum form an interesting group of quasi-one-dimensional compounds containing linear (or almost linear) chains of metal atoms. In many of these compounds charge-density-wave (CDW)-like distortions of the chains have been observed.

$NbTe_4$ and $TaTe_4$ are the only tellurides reported belonging to this group. Their basic structure was determined by Selte & Kjekshus (1964) ($NbTe_4$) and Bjerkelund & Kjekshus (1964) ($TaTe_4$); this tetragonal structure consists of columns of MTe_4 (M = Nb, Ta), containing linear chains of metal atoms. A certain structural resemblance can be remarked with the compounds $(MX_4)_nY$ (M = Nb, Ta; X = S, Se; Y = Br, I; $n = 2, 3, 3{\cdot}33, 4$). The latter compounds consist of MX_4 chains separated by I^- ions. A number of these compounds were prepared and characterized by Gressier, Meerschaut, Guemas, Rouxel & Monceau (1984). However, unlike the structures of these compounds, the columns in $NbTe_4$ and $TaTe_4$ are linked to each other by Te–Te bonds, which should decrease the one-dimensional character. This was indeed found from band-structure calculations of $NbTe_4$ (Whangbo & Gressier, 1984). Nevertheless, the structure of $NbTe_4$ at room temperature was found to have an incommensurate modulation of the basic structure (Boswell, Prodan & Brandon, 1983; Böhm & Von Schnering, 1983; Mahy, Wiegers, Van Landuyt & Amelinckx, 1984). The structure determination showed the distortion to be mainly a longitudinal displacement of the Nb atoms (Böhm & Von Schnering, 1985; van Smaalen, Bronsema & Mahy, 1986). At about 50 K $NbTe_4$ undergoes a transition to a commensurately modulated structure (Eaglesham, Bird, Witners & Steeds, 1985); this structure can be described by a $2a \times 2a \times 3c$ supercell. A commensurate superstructure with the same periodicity had already been observed by Bjerkelund & Kjekshus (1964) for $TaTe_4$ at room temperature. In the present paper we report the superstructure of $TaTe_4$ in detail and compare it with the incommensurate structure of $NbTe_4$.

Bjerkelund & Kjekshus (1964) proposed space group $P4cc$ for the basic structure of $TaTe_4$. Several studies have appeared since, reporting different results for the symmetry of $TaTe_4$. From X-ray diffraction, Boswell *et al.* (1983) report $P4cc$ as the space group of the subcell. Using convergent-beam electron diffraction (CBED), Eaglesham *et al.* (1985) determined space group $P4/mcc$ for both the average structure and the superstructure. On the basis of a theoretical analysis, Walker (1985*a*,*b*) derives as possible space groups for the superstructure $P4cc$ and $P4/ncc$. In a more recent paper, Sahu & Walker (1985) find that space group $P4/ncc$ will give the most stable structure. In our analysis we arrive at space group $P4/mcc$ for the average structure and at space group $P4/ncc$ for the superstructure. The space groups will be discussed in more detail in § 4.

* Present address: Enka B.V. Research Institute Arnhem, Velperweg 76, PO Box 60, 6800 AB Arnhem, The Netherlands.

0108-7681/87/040305-09$01.50

2. Experimental

The preparation of the $TaTe_4$ crystals is described elsewhere (Mahy *et al.*, 1984).

Weissenberg photographs taken with monochromatized Cu $K\alpha_1$ radiation clearly show the presence of superstructure reflections indicating a doubling of the a axis and a tripling of the c axis. Examining the diffraction pattern of $TaTe_4$, we can distinguish three classes of reflections: strong reflections at the nodes of the reciprocal lattice of the subcell, weak reflections at positions $\mathbf{q}_1 = (\frac{1}{2}, \frac{1}{2}, \frac{2}{3})$ from the main reflections and still weaker reflections at positions $\mathbf{q}_2 = (\frac{1}{2}, 0, \frac{2}{3})$ and $\mathbf{q}_3 = (0, \frac{1}{2}, \frac{2}{3})$. We call the reflections at positions $\mathbf{q}_1$, $\mathbf{q}_2$ and $\mathbf{q}_3$ the satellite reflections. Very weak reflections at $(0, 0, \frac{1}{3})$ are considered to be the second-order satellites of $\mathbf{q}_1$, $\mathbf{q}_2$ and $\mathbf{q}_3$, which coincide. We maintain this indexing in our comparison with the diffraction patterns of $NbTe_4$, in which satellite reflections at positions $\mathbf{q} = (\frac{1}{2}, \frac{1}{2}, 0{\cdot}691)$ are observed (van Smaalen *et al.*, 1986), although the structure of $TaTe_4$ was determined on the basis of a $2a \times 2a \times 3c$ supercell. The diffraction patterns of $NbTe_4$ and $TaTe_4$ are schematically given in Fig. 1. Satellites at positions $(\frac{1}{2}, 0, 0)$, $(0, \frac{1}{2}, 0)$ and $(\frac{1}{2}, \frac{1}{2}, 0)$, *i.e.* third-order satellites, were too weak to be observed on the photographs.

The intensity measurements were performed using a bar-shaped crystal of dimensions 0·0399 (7) × 0·0535 (7) × 0·332 (4) mm (standard deviations in the last decimal place are given in parentheses), the longest edge being in the direction of the c axis. 17 807 reflections were measured on a four-circle κ diffractometer CAD-4F (Enraf–Nonius) with monochromatized Mo $K\alpha$ radiation using the θ–2θ scan technique. The maximum angle θ was 55°; indices, on the basis of the $2a \times 2a \times 3c$ supercell, were in the range $0 \le H \le 30$, $0 \le K \le 30$ and $0 \le L \le 47$.* Corrections were made for Lorentz and polarization effects and for absorption (Spek, 1983). The min. and max. transmission values are 0·07 and 0·25 respectively. However, most of the values are between 0·17 and 0·25, and the extremely low values occur only for a few reflections with high l value. In the refinements a parameter for isotropic secondary extinction was included. The different refinements yield values of about 2×10^{-4} (Tables 3 and 5). Equivalent reflections (Laue symmetry $4/mmm$) were averaged and systematic absences discarded, leaving 8353 independent reflections. Scattering factors were from Cromer & Mann (1968). Anomalous-dispersion-correction factors were taken from *International Tables for X-ray Crystallography* (1974). Reflections with $F < 3\sigma(F)$ ('less thans') were omitted in the calculations, which were performed using the *XRAY* system (Stewart, Machin, Dickinson, Ammon, Heck & Flack, 1976). All third-order satellites were 'less than' and hence were not used in the refinements. The numbers of the different types of reflections are given in Table 1.*

* As for $NbTe_4$ (van Smaalen *et al.*, 1986), Miller indices for the subcell are given by lower-case letters h, k, l, those for the large cell by capital letters.

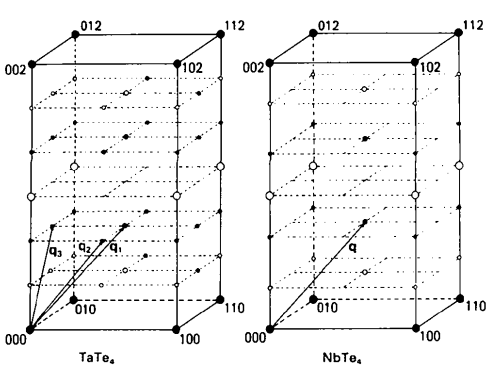

Fig. 1. The diffraction patterns of $TaTe_4$ and $NbTe_4$. Main reflections, first- and second-order satellites are shown. The different radii of the spots indicate different intensities. Open circles are systematically extinct reflections by the presence of the c-glide planes.

Table 1. *The number of measured unique reflections*

	Measured	$F > 3\sigma(F)$
Main reflections	961	916
$\mathbf{q}_1$ satellites	1849	1634
$\mathbf{q}_2$ and $\mathbf{q}_3$ satellites	3686	2702
Second-order satellites	1857	1171
Total	8353	6422

Table 2. *Lattice parameters* (Å) *of the average structure*

	This work	Bjerkelund & Kjekshus (1964)	Boswell *et al.* (1983)
a	6·5154 (5)	6·514	6·513
c	6·8118 (2)	6·809	6·812

For the average structure, systematic absences are found for the reflections hhl and $h0l$ with l = odd. Possible space groups for the average structure are then $P4cc$ and its centrosymmetric counterpart $P4/mcc$. For the complete structure no additional systematic absences could be detected, except for the third-order satellites all being less thans.

The lattice parameters of the subcell were determined from 25 high-order reflections, measured on the diffractometer. They are in good agreement with the values reported in the literature (Table 2).

3. Structure determination

From the diffraction pattern there are two possible space groups for the average structure: $P4cc$ and

* Lists of structure factors have been deposited with the British Library Document Supply Centre as Supplementary Publication No. SUP 43705 (148 pp.). Copies may be obtained through The Executive Secretary, International Union of Crystallography, 5 Abbey Square, Chester CH1 2HU, England.

Table 3. *Final parameters for the average structure after refinement on main reflections only*

Standard deviations in the last decimal place are given in parentheses. Temperature tensor components U_{ij} (Å^2) are defined by the formula $\exp(-2\pi^2\sum_i\sum_j U_{ij}h_ih_ja_i^*a_j^*)$.

		P4/mcc	*P4cc*
Ta	z	$\frac{1}{4}$	0·2380 (9)
	$U_{11}=U_{22}$	0·0060 (2)	0·0060 (2)
	U_{33}	0·076 (1)	0·073 (1)
Te	x	0·1438 (1)	0·1439 (1)
	y	0·3274 (1)	0·3274 (1)
	U_{11}	0·0189 (3)	0·0189 (4)
	U_{22}	0·0124 (3)	0·0124 (3)
	U_{33}	0·0110 (3)	0·0111 (3)
	U_{12}	0·0043 (2)	0·0043 (2)
	U_{13}	0	−0·0023 (7)
	U_{23}	0	−0·0023 (7)
Secondary extinction parameter		$2{\cdot}16\,(7)\times10^{-4}$	$2{\cdot}03\,(7)\times10^{-4}$

P4/mcc (§ 2). We refined the average structure in both space groups starting from the values determined by Bjerkelund & Kjekshus (1964). In *P4cc* the z coordinate of Te was kept zero to fix the origin. The results of both refinements are summarized in Table 3 and in Fig. 2. With a correction for secondary extinction, which appeared to be an important effect, the refinements yielded R_F factors of 0·079 and 0·082 for *P4cc* (12 parameters) and *P4/mcc* (9 parameters), respectively. Although the differences between the two refinements seem significant, particularly if we consider the large difference in the z coordinate of Ta (Table 3), we have to be careful. The very large value of the tensor element U_{33} of Ta, simulating the displacements in the z direction, may conceal the correct value of the z parameter of the Ta atoms in the average structure. Likewise, the values of the tensor elements of Te indicate that their shifts from the average position are mainly in the *ab* plane, thus introducing uncertainties in the x and y coordinates of the average position of the Te atoms. We conclude that the determination of the space group of the subcell is not possible at this stage. As will follow from the determination of the complete structure, the differences between the two refinements are indeed artificial; the space group of the average structure was found to be *P4/mcc*.

Inspection of the diffraction pattern of the $2a\times 2a\times 3c$ superstructure showed that the Laue symmetry and the extinction rules are the same as for the average structure. Because the third-order satellites are all 'less thans', we can deduce the additional extinction rule $H=2n+1$ and $K=2m+1$ for reflections HKL with $L=3p$ (n, m, p integer). However, there is no three-dimensional space group which explains these systematic absences. A possible space group is *P4/ncc* if we restrict the additional extinction rule to $H+K=2n+1$ for reflections $HK0$. If this extinction rule is disregarded, space groups *P4cc* and *P4/mcc* are also possible.

The determination of the superstructure was accomplished in two steps. The first step was the structure determination of what we will call the 'diagonal cell' (with edges $a\sqrt{2}\times a\sqrt{2}\times 3c$) using the main reflections, satellites $\mathbf{q}_1$ and second-order satellites. Further refinement of this result in the $2a\times 2a\times 3c$ supercell was the second step.

The intensities of satellites $\mathbf{q}_1$ are about three times as large as the intensities of satellites $\mathbf{q}_2$ and $\mathbf{q}_3$. This means that the main distortion can be determined from satellites $\mathbf{q}_1$. If we neglect satellites $\mathbf{q}_2$ and $\mathbf{q}_3$ the situation is analogous to that of $NbTe_4$. Following the same procedure as used for $NbTe_4$ (van Smaalen *et al.*, 1986) but now with the commensurate modulation wave vector $\mathbf{q}_1=(\frac{1}{2},\frac{1}{2},\frac{2}{3})$, we found a starting model. Main reflections and $\mathbf{q}_1$ satellites define the 'diagonal cell', in which the model was further refined. Second-order satellites $(0,0,\frac{1}{3})$ were also included. Satisfactory results were obtained for space groups *P4cc* and *P4/mcc*: R_F factors were 0·067 and 0·081, respectively. The R_F factors for the different reflection types are given in Table 4. The results of the refinements in the two space groups are schematically shown in Fig. 3 for the Ta atoms only. The arrangement of the Ta atoms in column *A* (and in *B*) (for the notation see Fig. 2) is essentially the same in both cases: the formation of triplets of atoms is evident. The results for columns *C* (and *D*) differ remarkably: in the centrosymmetric space group we find alternating pairs and single atoms while in the non-centrosymmetric space group triplets are found again. The hatched atoms in Fig. 3 have large values of the tensor element U_{33} [0·119 (3) Å^2]. This indicates a large additional modulation of these atoms resulting in the satellites $\mathbf{q}_2$ and $\mathbf{q}_3$. As in the case of the average structure the 'improvement' of *P4cc* over *P4/mcc* is again an artifact originating in the additional modulation. The true symmetry of the 'diagonal cell' is described by space group *P4/mcc* as will follow from

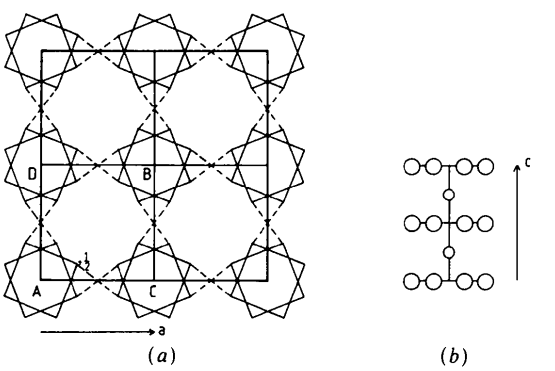

Fig. 2. (*a*) Projection of the average structure along the *c* axis. Several unit cells are shown. The columns which are of interest for the superstructure are indicated. Dotted lines indicate the Te–Te bonds. (*b*) Projection of the $TaTe_4$ chain in the subcell on the *ac* plane. Large circles are Te atoms, small circles are Ta atoms.

Table 4. *R_F values for the various reflection types in intermediate and final refinements*

Reflection type	Subcell *P4/mcc*	Subcell *P4cc*	Diagonal cell *P4/mcc*	Diagonal cell *P4cc*	Final *P4cc*	Final *P4/ncc*
Main	0·082	0·079	0·038	0·035	0·030	0·032
$\mathbf{q}_1$ satellites	—	—	0·088	0·063	0·049	0·051
Second-order satellites	—	—	0·245	0·229	0·154	0·187
$\mathbf{q}_2$ and $\mathbf{q}_3$ satellites	—	—	—	—	0·097	0·110
Overall	0·082	0·079	0·081	0·067	0·063	0·064
Number of parameters	9	12	41	72	141	72

the determination of the complete superstructure. Atoms in column *A* (and *B*) do not have abnormally large temperature factors. From this we conclude that in the superstructure these columns are equivalent through the fourfold axes which, therefore, must lie at columns *C* and *D*. Since the hatched Ta atoms lie on special positions 2(*a*), $(0, 0, \frac{1}{4})$ and $(0, 0, \frac{3}{4})$ in space group *P4/mcc*, and they seem to have opposite displacements in columns *C* and *D*, space group *P4/mcc* cannot describe the symmetry of the complete superstructure. Nevertheless, some refinements were tried using this space group but were not successful.

A model was built based on the assumptions mentioned above. In this model Ta atoms form triplets on all columns; a phase shift of 1/3 between triplets in neighbouring columns is assumed. In addition, a few Te atoms were shifted accordingly. The refinement, carried out in space group *P4cc*, converged smoothly to a final R_F value of 0·063, using 141 parameters. Careful analysis of the results showed the presence of a pseudo-centre of symmetry at the positions of the centres of symmetry in space group *P4/ncc*. A refinement in the latter space group yielded an R_F factor of 0·064, using 72 parameters. Comparing the two results, we noticed that there were no significant differences between coordinates in *P4cc* and *P4/ncc* within experimental accuracy. The symmetry of the superstructure of $TaTe_4$ is therefore given by space group *P4/ncc*. The final parameters are listed in Table 5. The R_F factors of the different types of reflections are given in Table 4. The differences in R_F factors between the reflection types are caused by their relative intensities. Inspection of the structure-factor list shows that the values of $\Delta|F| = ||F_{obs}| - |F_{calc}||$ are of the same magnitude for all reflection types. Consequently, the relative error is larger for a reflection type with relatively low intensity.

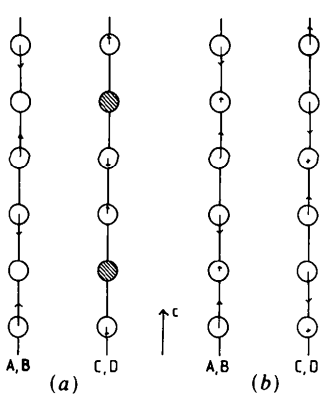

Fig. 3. Displacements (×5) of the Ta atoms in columns *A* and *C* as derived from the refinements of the diagonal cell in (*a*) *P4/mcc* and (*b*) *P4cc*. For explanation see text.

4. Symmetry

As was mentioned in the *Introduction*, several space groups were proposed for the subcell and for the supercell of $TaTe_4$. From our X-ray diffraction study we conclude that the space group of the superstructure is *P4/ncc* within experimental error; this means that the average structure can be described in space group *P4/mcc*. In this section we will discuss how, in our opinion, the different proposals for the space groups could arise.

Bjerkelund & Kjekshus (1964) and Boswell *et al.* (1983) reported space group *P4cc* for the average structure. Their results were based on refinement of the main reflections only. Using convergent-beam electron diffraction (CBED), Eaglesham *et al.* (1985) concluded that the space group of the subcell was *P4/mcc*. Our refinements on the main reflections only showed that a decision between space groups *P4cc* and *P4/mcc* is not possible on that basis. The calculation of the average structure from the complete superstructure shows that the space group of the subcell is *P4/mcc*. Therefore, the (small) improvement of the refinement of the subcell in *P4cc* over that in *P4/mcc* is caused by an improper account of the modulation; the differences found have no structural significance.

The situation for the superstructure is more complicated. Since the space group of a superstructure is a subgroup of that of the average structure, the choice of space group *P4cc* for the subcell necessarily leads to space group *P4cc* for the supercell (or even to one of lower symmetry). If the space group of the subcell is *P4/mcc*, possible space groups of the superstructure are *P4/mcc*, *P4/ncc* and *P4cc* (or one of lower symmetry). Using Landau theory, Sahu & Walker (1985) and Walker (1985*a*,*b*) predict space group *P4/ncc*. With CBED, Eaglesham *et al.* (1985) determine *P4/mcc* as the space group of the superstructure. In principle, the CBED technique allows one to establish

Table 5. *List of the final parameters of the superstructure of* $TaTe_4$, *space group P4/ncc*

The temperature factor is as defined in Table 3. Standard deviations are given in parentheses. Secondary-extinction parameter: $2{\cdot}25\,(2)\times10^{-4}$.

	Column*	Position†	x	y	z	U_{11}	U_{22}	U_{33}	U_{12}	U_{13}	U_{23}
Ta(1)	*A*	8(*e*)	0	0	0·09652 (4)	0·0064 (2)	0·0065 (2)	0·0068 (2)	0·0002 (2)	0	0
Ta(2)	*A*	4(*a*)	0	0	$\frac{1}{4}$	0·0063 (2)	‡	0·0068 (3)	0·0000 (3)	0	0
Ta(3)	*D*	4(*c*)	0	$\frac{1}{2}$	0·41827 (5)	0·0065 (2)	‡	0·0056 (3)	0	0	0
Ta(4)	*D*	4(*c*)	0	$\frac{1}{2}$	0·26351 (6)	0·0063 (2)	‡	0·0070 (3)	0	0	0
Ta(5)	*D*	4(*c*)	0	$\frac{1}{2}$	0·07030 (5)	0·0064 (2)	‡	0·0072 (3)	0	0	0
Te(1)	*A*	16(*g*)	0·0611 (1)	0·1579 (1)	−0·0003 (1)	0·0090 (4)	0·0095 (4)	0·0085 (3)	−0·0006 (3)	−0·0004 (4)	−0·0005 (3)
Te(2)	*C*	16(*g*)	0·5802 (1)	0·1655 (1)	0·0017 (1)	0·0097 (4)	0·0077 (3)	0·0096 (4)	−0·0007 (3)	−0·0001 (4)	−0·0000 (3)
Te(3)	*A*	16(*g*)	0·1656 (1)	0·0789 (1)	0·1686 (1)	0·0076 (3)	0·0096 (4)	0·0092 (4)	−0·0005 (3)	0·0005 (3)	−0·0003 (4)
Te(4)	*B*	16(*g*)	0·6665 (1)	0·5747 (1)	0·1697 (1)	0·0076 (3)	0·0086 (3)	0·0095 (4)	0·0001 (2)	0·0000 (3)	0·0000 (3)
Te(5)	*C*	16(*g*)	0·6687 (1)	0·0700 (1)	0·1633 (1)	0·0083 (4)	0·0098 (3)	0·0085 (4)	−0·0005 (2)	0·0003 (3)	0·0001 (3)
Te(6)	*D*	16(*g*)	0·1561 (1)	0·5648 (1)	0·1675 (1)	0·0102 (4)	0·0085 (3)	0·0088 (3)	−0·0008 (3)	0·0008 (3)	0·0006 (3)

* The letters indicate the column in which the atom resides (see Fig. 2); equivalent atoms also reside in another column.
† Positions according to the first setting of *P4/ncc*.
‡ $U_{22}=U_{11}$ by symmetry.

the point symmetry of the structure, as well as the translation parts of the operators of the space group. This makes it possible to distinguish between the three space groups *P4/mcc*, *P4/ncc* and *P4cc*. Eaglesham *et al.* (1985) observed point symmetry *4/mmm* allowing space groups *P4/mcc* and *P4/ncc*. They rejected *P4/ncc* because they found one reflection violating the extinction rule for the *n* glide (Bird, Eaglesham, Withers, McKernan & Steeds, 1984). We rejected space group *P4/mcc* from structural arguments (§ 3). As to the reflections violating the extinctions of the *n* glide, we conclude that the (apparent) deviation from the *n* glide exhibited in the diffraction pattern by intensity at the nodes where the reflections should be systematically absent does not show up in the reflections used for the determination of the point group. If the *n* glide is indeed absent, the symmetry of the superstructure has to be described by space group *P4cc*. In § 3 we show that this is possible. However, our refinements show that, within experimental error, the space group is *P4/ncc*. Furthermore, we found by electron diffraction that the reflections violating the *n* glide are heavily affected by dynamic effects, as was also observed by Eaglesham *et al.* (1985). Hence, we conclude that the superstructure of $TaTe_4$ is properly described by space group *P4/ncc*. Note that the distinction between space groups *P4cc*, *P4/mcc* and *P4/ncc* could only be made after determining the complete superstructure.

5. Discussion

The average structure of $TaTe_4$ is characterized by chains of composition $TaTe_4$ along the tetragonal *c* axis. Ta atoms are placed on the fourfold axis at equal distances of 3·406 Å ($=\frac{1}{2}c$). Each Ta atom is surrounded by eight Te atoms in a square anti-prismatic configuration (Fig. 2). Closest approaches between Te atoms in the same column are the edges of the Te squares (3·287 Å). The closest distance between Te atoms in adjacent columns is 2·928 Å, indicating that Te–Te bonds between neighbouring columns are present. The Ta–Te bonding distance is 2·882 Å.

The average (basic) structure of $TaTe_4$ is commensurately modulated in such a way that a $2a\times2a\times3c$ superstructure is formed. In this superstructure we find four $TaTe_4$ columns *A*, *B*, *C* and *D* (Fig. 2). These are not all crystallographically independent: columns *A* and *B* are related by fourfold axes at $\frac{1}{2}, 0, z$ and $0, \frac{1}{2}, z$ and columns *C* and *D* are equivalent by a centre of symmetry. Thus, there are two independent types of columns present in the structure. The modulation with the largest amplitude is that on the Ta atoms. Displacements are such that triplets of Ta atoms are formed in each column. This is shown in Fig. 4. In order to keep the Ta–Te and Te–Te bond distances as constant as possible, there is a phase shift of $\frac{1}{3}$ between triplets in neighbouring columns. The formation of triplets leads to shortening and

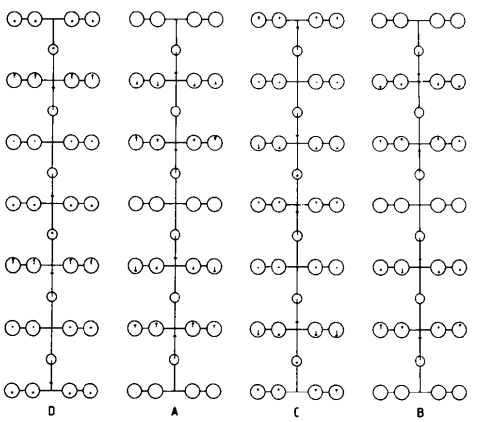

Fig. 4. Displacements (×5) of the atoms on the various columns in the *z* direction as found in the final refinement in *P4/ncc*.

Table 6. *Important interatomic distances in* $TaTe_4$; d_{av} *gives the value of the distance in the average structure*

(*a*) Ta–Ta distances along the *c* axis ($d_{av} = 3{\cdot}406$ Å)

Column		*d* (Å)
A, *B*	Ta(1)–Ta(2)	3·1365 (8)
A, *B*	Ta(1)–Ta(1)	3·945 (1)
C, *D*	Ta(3)–Ta(4)	3·162 (2)
C, *D*	Ta(3)–Ta(5)	3·107 (2)
C, *D*	Ta(4)–Ta(5)	3·948 (2)

(*b*) Length of the edges of the various Te 'squares' ($d_{av} = 3{\cdot}287$ Å)

Column	Type	$\bar{z}$	*d* (Å)	$\bar{d}$ (Å)
A	*a*	0	3·120 (1)	
A	*b*	$\frac{1}{6}$	3·381 (2)	3·372
A	*b*	$\frac{1}{6}$	3·363 (2)	
C	*b*	0	3·390 (1)	
C	*b*	$\frac{1}{6}$	3·367 (2)	
C	*a*	$\frac{1}{3}$	3·115 (2)	

(*c*) Te–Te bond distances in $TaTe_4$ ($d_{av} = 2{\cdot}929$ Å)

Column 1	Column 2		$\bar{z}$	*d* (Å)
A	*C*	Te(1)–Te(2)	0	2·947 (2)
A	*C*	Te(3)–Te(5)	$\frac{1}{6}$	2·905 (2)
A	*D*	Te(4)–Te(6)	$\frac{1}{6}$	2·942 (2)

(*d*) Ta–Te bonding distances ($d_{av} = 2{\cdot}882$ Å)

Column	Type		*d* (Å)
A	1	Ta(1)–Te(1)	2·955 (2)
A	1	Ta(1)–Te(1)	2·964 (2)
A	2	Ta(1)–Te(3)	2·807 (2)
A	2	Ta(1)–Te(4)	2·809 (2)
A	3	Ta(2)–Te(3)	2·913 (3)
A	3	Ta(2)–Te(4)	2·889 (2)
C	3	Ta(3)–Te(2)	2·901 (2)
C	3	Ta(3)–Te(5)	2·906 (2)
C	2	Ta(4)–Te(5)	2·812 (2)
C	1	Ta(4)–Te(6)	2·950 (2)
C	1	Ta(5)–Te(6)	2·966 (2)
C	2	Ta(5)–Te(2)	2·813 (2)

lengthening of the Ta–Ta distances with respect to the basic structure. The average value of the shorter distances is 3·13 Å, corresponding with a displacement of 0·27 Å of the outer Ta atoms of each triplet. The corresponding lengthened distance is 3·95 Å. All important distances are given in Table 6.

In response to the displacements of the Ta atoms two types of Te 'squares' are formed (Fig. 5): one-third of the squares have contracted (type *a*), two-thirds have expanded (type *b*) relative to the average. Columns *A* and *B* have a twofold axis only in the superstructure, therefore the Te squares of the average structure may distort to rectangles in the superstructure, as is indeed found (Fig. 5). Because this deviation is small we shall not discusss it here. The contracted squares are found between Ta atoms displaced away from each other, the expanded squares between the Ta atoms forming a triplet. The lengths of the edges of the Te squares are given in Table 6(*b*). The edges of particularly the contracted Te squares are much shorter than corresponds to the Te–Te van der Waals distance, indicating considerable interaction between the Te_2^{2-} groups. This interaction causes the Te–Te bonds within a pair to be somewhat longer than is usual for Te_2^{2-} groups [*e.g.* 2·761 Å in $ZrTe_3$ (Furuseth, Brattås & Kjekshus, 1975)]. There is hardly any variation in the Te–Te bond distance (Table 6*c*). To keep the Te–Te bonding distance as constant as possible seems to be a boundary condition for the structure. It depends on the relative position of the types of Te squares how this condition is fulfilled. At $\bar{z} = 0$ (Fig. 5*a*) types *a* are in columns *A* and *B* and are separated by types *b* in *C* and *D*. We here observe parallel shifts of the Te pairs. At $\bar{z} = \frac{1}{6}$ and $\bar{z} = \frac{1}{3}$ (Figs. 5*b* and *c*) this is only partly possible: where types *a* and *b* are neighbours a parallel shift is observed; where types *b* are neighbours the Te–Te distance is kept constant by a rotation accompanying the shifts.

From Table 6(*d*) we can derive that the Ta–Te distances are not quite constant. There are three types of Ta–Te distances found in each column: (1) elongated, (2) shortened and (3) almost unchanged Ta–Te bonds relative to the average structure. Type 1 distances are found between Ta and Te atoms in type *a* 'squares', type 2 distances between the same Ta atoms and Te atoms in type *b* 'squares', and type 3 distances for Ta atoms sandwiched between type *b* Te 'squares'.

There is obviously a large coherence between the displacements of the Ta and Te atoms. This was also found in the incommensurately modulated structure of $NbTe_4$ (van Smaalen *et al.*, 1986). In Fig. 6 we compare the important distances of $TaTe_4$ (Table 6)

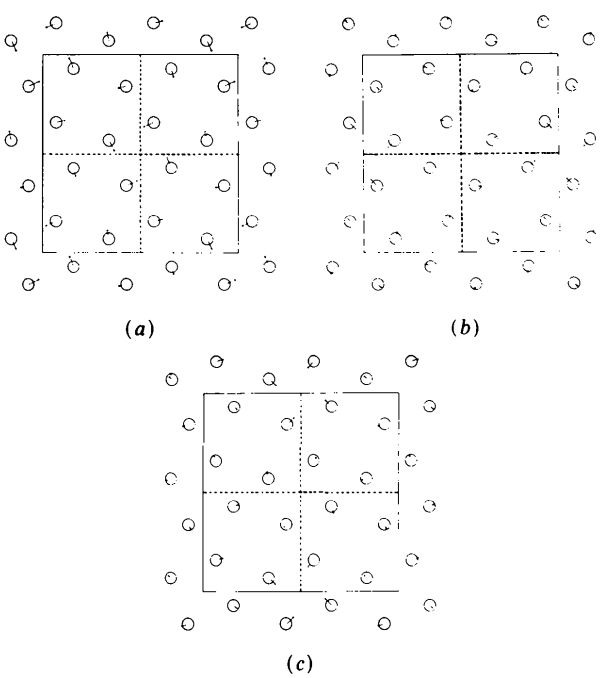

Fig. 5. Projection of the final structure along c. The displacements of the Te atoms in the *ab* plane are indicated by arrows; the actual displacements are one-fifth of the length of the arrows. (*a*) At $\bar{z} = 0$; (*b*) at $\bar{z} = \frac{1}{6}$ and (*c*) at $\bar{z} = \frac{1}{3}$.

with the corresponding distances in $NbTe_4$. In this figure the interatomic distances are given as a function of t, defined by $\bar{x}_4 = \mathbf{q}.\mathbf{r}_0 + t$; here $\bar{x}_4$ is the fourth coordinate in the four-dimensional description of the structure of $NbTe_4$ (van Smaalen *et al.*, 1986) and $\mathbf{r}_0$ the position of an atom in the average structure. For $NbTe_4$, $\mathbf{q} = (0, 0, 0{\cdot}691)$ [after transformation of the subcell (van Smaalen *et al.*, 1986)]; for $TaTe_4$, we take $\mathbf{q} = (0, 0, \frac{2}{3})$. For example, distances between the same atoms, shifted by n unit cells (of the average structure) along $\mathbf{c}$, are given by $t = n\mathbf{q}.\mathbf{c}$ (mod 1). For an incommensurate modulation all values of t are possible. This corresponds with the solid lines in Fig. 6 which give the interatomic distances in $NbTe_4$. Because of the commensurate character of the modulation in $TaTe_4$ only certain values of t are possible: $t = \varphi, \frac{1}{3}+\varphi, \frac{2}{3}+\varphi$ (mod 1); φ is a phase shift which is determined by the actual three-dimensional structure (Bronsema & Mahy, 1987; van Smaalen, 1985). If we take the origin at $(0, \frac{1}{2}, 0)$ (column D) and apply a phase shift of $\frac{1}{6}$ for this column and take into account the phase shift between neighbouring columns, we find close similarity between the modulations in $NbTe_4$ and $TaTe_4$.

The structure of $TaTe_4$ can be described as a (commensurately) modulated structure, just like the (incommensurate) structure of $NbTe_4$. The latter could be described by a 3+1-dimensional space group (van Smaalen *et al.*, 1986), following the approach of de Wolff, Janssen & Janner (1981) and Janner, Janssen & de Wolff (1983). One might expect that a similar approach is also possible for $TaTe_4$. This is currently under investigation, but we have some indications that a description of the structure using a superspace group could be favourable. In the first place, using space group $P4/ncc$, we could explain only a part of the observed extinction rule $H = 2n+1$ and $K = 2m+1$, for reflections HKL with $L = 3p$. With the final structure model (Table 5), the intensities of these reflections were calculated. They were of the order of the differences $|\Delta F|$ of the other reflections and are indeed 'less thans'. In the superspace-group approach it is possible that this extinction rule will be explained by symmetry. Secondly, it is noticed for the displacements of the Te atoms that, within experimental error, $\Delta x[\mathrm{Te}(3)] + \Delta x[\mathrm{Te}(4)] = -\Delta y[\mathrm{Te}(1)]$, $\Delta x[\mathrm{Te}(5)] + \Delta x[\mathrm{Te}(6)] = -\Delta y[\mathrm{Te}(2)]$ and similar relations hold for the y coordinates. We expect that these observations can be explained using the superspace-group approach.

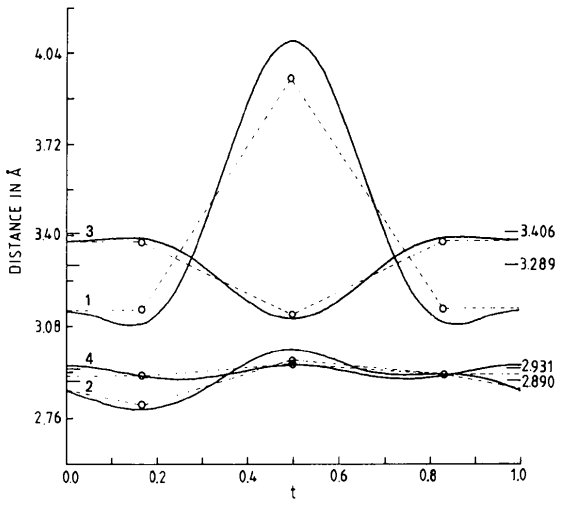

Fig. 6. Comparison between important distances in $NbTe_4$ and $TaTe_4$. For explanation see text. (1) M–M distance; (2) M–Te distance; (3) Te–Te distance on the same column (edge of square); and (4) Te–Te distance between neighbouring columns (Te_2 pairs). Average distances for $TaTe_4$ are indicated.

A compound related to $NbTe_4$ and $TaTe_4$ is VS_4, which also has a structure with linear chains of metal atoms (Allmann, Baumann, Kutoglu, Rösch & Hellner, 1964). However, the coordination of the metal atoms by the dichalcogen groups is different in VS_4 from that in $NbTe_4$ and $TaTe_4$. In $NbTe_4$ and $TaTe_4$ the Te_2^{2-} groups are bound to the metal atoms of two chains. The coordination is such that there is overlap between the empty metal d orbitals and the filled π_g^* orbitals of the Te_2^{2-} groups. In VS_4 the S_2^{2-} groups are coordinated edge-on to one chain of metal atoms. This coordination does not have overlap between the metal d orbitals and the S_2^{2-} π_g^* orbitals.

The $NbTe_4$ type of coordination [or the related pyrite or marcasite type of coordination, *cf.* van Bruggen (1982)] is stabilized with respect to the edge-on coordination, if the resulting d, p mixing is large enough. That is, if the metal d orbitals and the X_2^{2-} (X = S, Te) π_g^* orbitals are close enough in energy. For VS_4 the energy difference is large, as follows from XPS (Folmer, 1980). No stabilization of the $NbTe_4$ type of coordination is expected in this compound. For $NbTe_4$ and $TaTe_4$, consideration of the electronegativity suggests this energy difference to be less than in VS_4. The experimentally determined $NbTe_4$ type of coordination may be ascribed to stabilization by d, p mixing. A recording of the XPS spectra for these compounds would be interesting to measure this effect.

As follows from the structure determinations, $TaTe_4$, $NbTe_4$ (van Smaalen *et al.*, 1986) and the isoelectronic compound VS_4 (Allmann *et al.*, 1964) have a high one-dimensional character. Along the chains, the interatomic distances between the metal atoms (Ta, Nb, V) are short compared with the van der Waals radii. Between the chains the distances between the atoms are too long for any direct metal–metal bonding. Such a high one-dimensional character is indeed found in band-structure calculations for $NbTe_4$ (Whangbo & Gressier, 1984). This suggests that the observed distortion might be due to the Peierls (1955) mechanism, which states that the distortion occurs with a wave vector equal to twice the Fermi

wave vector of the electron band. The difference in modulation wave vector for these three compounds can then be explained by the differences in the band structure. However, the band-structure calculations available (Bullet, 1984; Whangbo & Gressier, 1984) are not detailed enough to make such a comparison possible.

The Peierls mechanism assumes the distortion to be an intrinsic property of one chain. Therefore, it does not explain the phase relationship between the distortions on different chains. This phase relation can be obtained from a Landau free-energy expansion with the amplitude of the modulation wave as order parameters and with some model for the interaction between different columns (Sahu & Walker, 1985; Walker, 1985*a*).

To describe the distortion in one column, Sahu & Walker (1985*a*,*b*) used a single complex order parameter $\Psi^{(n)} = \alpha \exp(i\varphi_n)$, with its amplitude independent of the column n. They assumed the distortion to take place with the symmetry of the Γ_2 irreducible representation of the little group of $k = \tau c^*$ (τ is $\frac{1}{3}$ and 0·31 for $TaTe_4$ and $NbTe_4$ respectively) in the basic structure space group $P4/mcc$. For a suitable choice of the phases φ_n for the four columns $n = A$, B, C, D (Fig. 2), this function describes the main part of the distortion. The remaining part of the distortion can be described with functions with a symmetry of Γ_2 ($k = 2\tau c^*$) and, for $TaTe_4$ only, with a symmetry of Γ_4 ($k = \frac{1}{3}c^*$).

For the commensurate modulation $q = \frac{2}{3}c^*$ ($TaTe_4$), the free energy for a single column is a minimum for $\varphi_n = (2\pi/3)m_n \pmod{2\pi}$, $m_n = 0, \pm 1$ (Sahu & Walker, 1985). For $NbTe_4$, the incommensurateness of the modulation ensures that the free energy is independent of the phase φ_n.

To determine the phase relation between the distortions of different columns, Sahu & Walker (1985) assumed an interaction of the form

$$F_{nm} = \tfrac{1}{4}G \int \mathrm{Re}\,[\Psi^{(m)}\Psi^{(n)*}]\,\mathrm{d}z,$$

where n and m label the columns and both nearest-neighbour (G_1) and next-nearest-neighbour (G_2) interactions are taken into account. Assuming not more than four different columns on a $2a \times 2a$ lattice (Fig. 2), Sahu & Walker (1985) derived the values for the phases which give a minimum of the free energy for the commensurate case of $TaTe_4$. Several solutions are obtained, depending on the values of G_1 and G_2. The solution compatible with the structure determination in this work is

$$\varphi^A = \varphi^B = 0, \qquad \varphi^C = \phi, \qquad \varphi^D = -\phi.$$

For small values of G_1 and G_2 they find that $\varphi \simeq 2/3\pi$, where the precise value depends on the values of G_1 and G_2.

If we assume a similar interaction in $NbTe_4$, a similar solution is expected in this compound. However, the modulation is now incommensurate, leading to a minimum for the free energy for $\varphi = 0$ or $\varphi = \pi$. The latter value leads to idental columns C and D. The unit cell than has a $\sqrt{2}a \times \sqrt{2}a$ basal plane, with space group $W^{P4/mcc}_{1\ 111}$ (Walker, 1985*b*), in accordance with the structure determined with X-ray diffraction (van Smaalen *et al.*, 1986).

In conclusion, it can be said that Landau-theory calculations as carried out by Sahu & Walker (1985) are able to explain the distortion occurring in $NbTe_4$ and $TaTe_4$. Moreover, Landau theory predicts accurately the different phase relations between neighbouring columns for the case of commensurate modulation ($TaTe_4$) and incommensurate modulation ($NbTe_4$).

6. Concluding remarks

The main difficulty in the present crystal structure analysis of $TaTe_4$ was the determination of the space group. From our X-ray data we concluded that the superstructure is best described in space group $P4/ncc$ and the average structure in $P4/mcc$. A more convenient description may probably be achieved by a superspace group.

The superstructure of $TaTe_4$ can be regarded as a commensurately modulated structure. The nature of the modulation is such that triplets of Ta atoms are formed. Te atoms are found to respond to the displacements, keeping the pair Te–Te distances as constant as possible. A good resemblance was found between the structure of $TaTe_4$ and the incommensurately modulated structure of $NbTe_4$. When one chain is considered, the modulations on $NbTe_4$ and $TaTe_4$ are much alike. The differences between these compounds are mainly given by the value of $\mathbf{q}_z$ and by the different phase shifts between neighbouring columns.

The different phase relationships between neighbouring columns in $TaTe_4$ and $NbTe_4$ respectively could be explained by Landau theory based on the calculations of Sahu & Walker (1985). It appeared that the difference is completely determined by the z component of the modulation wave vector being commensurate in $TaTe_4$ and incommensurate in $NbTe_4$.

We thank A. Looyenga-Vos for valuable discussions and A. L. Spek and R. Olthof-Hazekamp for their help in the determination of the absorption correction.

This investigation was supported in part by The Netherlands Foundation for Chemical Research (SON) with financial aid from the Netherlands Organization for the Advancement of Pure Research (ZWO) which is gratefully acknowledged.

References

ALLMANN, R., BAUMANN, L., KUTOGLU, A., RÖSCH, H. & HELLNER, E. (1964). *Naturwissenschaften*, **51**, 263-264.

BIRD, D. M., EAGLESHAM, D. J., WITHERS, R. L., MCKERNAN, S. & STEEDS, J. W. (1984). *Proc. International Conference on Charge Density Waves in Solids, Budapest*, 1984, edited by GY. HUTIRAY & J. SOLYOM, pp. 23-32. Berlin: Springer-Verlag.

BJERKELUND, E. & KJEKSHUS, A. (1964). *J. Less-Common Met.* **7**, 231-234.

BÖHM, H. & VON SCHNERING, H. G. (1983). *Z. Kristallogr.* **162**, 26-27.

BÖHM, H. & VON SCHNERING, H. G. (1985). *Z. Kristallogr.* **171**, 41-64.

BOSWELL, F. W., PRODAN, A. & BRANDON, J. K. (1983). *J. Phys. C*, **16**, 1067-1076.

BRONSEMA, K. D. & MAHY, J. (1987). In preparation.

BRUGGEN, C. F. VAN (1982). *Ann. Chim. (Paris)*, **7**, 171.

BULLET, D. W. (1984). *J. Phys. C*, **17**, 253-257.

CROMER, D. T. & MANN, J. B. (1968). *Acta Cryst.* A**24**, 321-324.

EAGLESHAM, D. J., BIRD, D., WITNERS, R. L. & STEEDS, J. W. (1985). *J. Phys. C*, **18**, 1-11.

FOLMER, J. C. W. (1980). Unpublished.

FURUSETH, S., BRATTÅS, L. & KJEKSHUS, A. (1975). *Acta Chem. Scand. Ser. A*, **29**, 623.

GRESSIER, P., MEERSCHAUT, A., GUEMAS, L., ROUXEL, J. & MONCEAU, P. (1984). *J. Solid State Chem.* **51**, 141-151.

International Tables for X-ray Crystallography (1974). Vol. IV. Birmingham: Kynoch Press. (Present distributor D. Reidel, Dordrecht.)

JANNER, A., JANSSEN, T. & DE WOLFF, P. M. (1983). *Acta Cryst.* A**39**, 658-666.

MAHY, J., WIEGERS, G. A., VAN LANDUYT, J. & AMELINCKX, S. (1984). *Mater. Res. Soc. Symp. Proc.* **21**, 181-188.

PEIERLS, R. E. (1955). *Quantum Theory of Solids*. Oxford: Clarendon Press.

SAHU, D. & WALKER, M. B. (1985). *Phys. Rev. B*, **32**, 1643-1648.

SELTE, K. & KJEKSHUS, A. (1964). *Acta Chem. Scand.* **18**, 690-696.

SMAALEN, S. VAN (1985). PhD Thesis, Univ. of Groningen.

SMAALEN, S. VAN, BRONSEMA, K. D. & MAHY, J. (1986). *Acta Cryst.* **42**, 43-50.

SPEK, A. L. (1983). Proc. 8th Eur. Crystallogr. Meet., Liège, Belgium.

STEWART, J. M., MACHIN, P. A., DICKINSON, C. W., AMMON, H. L., HECK, H. & FLACK, H. (1976). The *XRAY*76 system. Tech. Rep. TR-446. Computer Science Center, Univ. of Maryland, College Park, Maryland.

WALKER, M. B. (1985*a*). *Can. J. Phys.* **63**, 46-49.

WALKER, M. B. (1985*b*). Private communication.

WHANGBO, M.-H. & GRESSIER, P. (1984). *Inorg. Chem.* **23**, 1228-1232.

WOLFF, P. M. DE, JANSSEN, T. & JANNER, A. (1981). *Acta Cryst.* A**37**, 625-636.

Acta Cryst. (1987). B**43**, 313-318

A Crystallographic Study of the Phase Transition in Rubidium Dihydrogen Citrate

BY MATTHEW HOLCOMB, MARIANNA STRUMPEL, WILLIAM M. BUTLER AND CHRISTER E. NORDMAN

Department of Chemistry, University of Michigan, Ann Arbor, Michigan 48109, *USA*

(*Received* 8 *January* 1987; *accepted* 17 *February* 1987)

Abstract

$Rb^+.C_6H_7O_7^-$, $M_r = 275{\cdot}58$, monoclinic, $P2_1/a$, $a = 14{\cdot}903\ (2)$, $b = 9{\cdot}731\ (2)$, $c = 19{\cdot}220\ (3)$ Å, $\beta = 108{\cdot}62\ (2)°$, $V = 2641{\cdot}6\ (6)$ Å^3, $Z = 12$, $D_x = 2{\cdot}079$ g cm^{-3}, λ(Mo $K\alpha$) = 0·71069 Å, $\mu = 54{\cdot}8$ cm^{-1}, $F(000) = 1620$, $T = 295\ (2)$K. Bragg reflections with $l = 3n$ are stronger than those with $l \neq 3n$. In a phase transition at approximately 308 K the $l \neq 3n$ reflections vanish, giving a high-temperature cell with $a = 14{\cdot}917\ (3)$, $b = 9{\cdot}763\ (3)$, $c = 6{\cdot}423\ (2)$ Å, $\beta = 108{\cdot}54\ (2)°$, $V = 886{\cdot}8\ (3)$ Å^3, $Z = 4$, $D_x = 2{\cdot}064$ g cm^{-3}, $F(000) = 540$, $T = 323\ (3)$ K, corresponding to a reduced cell in $P2_1/n$, with $a = 14{\cdot}242\ (3)$, $b = 9{\cdot}763\ (3)$, $c = 6{\cdot}423\ (2)$ Å, $\beta = 96{\cdot}77\ (2)°$. The nature of the phase transition is revealed by the results of structure determinations of the low-temperature phase at 225 (3) K based on 4387 measured reflections with $|F_o| > 0$, and giving $R = 0{\cdot}0636$, and of the high-temperature phase at 323 (3) K, with 1710 measured reflections with $|F_o| > 0$ and $R = 0{\cdot}0398$. All O-bound H atoms in both structures participate in intermolecular hydrogen bonds, forming three-dimensional networks. In the low-temperature phase, the $c/3$ translational pseudosymmetry is broken by a 15° rotation of one of the three independent molecules. This is accompanied by a switch in the position of a hydrogen-bonding H from one O atom to the other in a terminal carboxyl group of the rotated citrate ion. The instability of the high-temperature phase at lower temperature can be qualitatively understood in terms of a close (C–)H···O contact, with H···O = 2·33 (3) Å. One of every three such contacts is removed by the rotation of one citrate ion; the other two contacts are relieved, to a lesser degree, by accompanying small shifts in the positions of the other citrate ions and the Rb^+ ions. A disorder exists in the position of one CH_2CO_2H group of the high-temperature structure, with the minor component approximating the rotated citrate ion in the low-temperature phase. Short hydrogen bonds, approximately in the x direction, with O···O distances 2·492 (6), 2·524 (6) and 2·502 (6) Å, link glide-plane-related molecules in the low-temperature phase. Upon deuteration, the length of the a axis of the low-temperature phase increases by 0·019 (3) Å.

0108-7681/87/040313-06$01.50